

Document downloaded from:

<http://hdl.handle.net/10251/182475>

This paper must be cited as:

Herweg, B.; Nellaiyappan, M.; Welter-Frost, AM.; Tran, T.; Mabry, G.; Weston, K.; Tobón, C.... (2021). Immuno-Electrophysiological Mechanisms of Functional Electrical Connections Between Recipient and Donor Heart in Patients With Orthotopic Heart Transplantation Presenting With Atrial Arrhythmias. *Circulation Arrhythmia and Electrophysiology*. 14(4):412-423. <https://doi.org/10.1161/CIRCEP.120.008751>



The final publication is available at

<https://doi.org/10.1161/CIRCEP.120.008751>

Copyright Ovid Technologies Wolters Kluwer -American Heart Association

Additional Information

Immuno-Electrophysiological Mechanisms of Functional Electrical Connections Between Recipient and Donor Heart in Patients with Orthotopic Heart Transplantation Presenting with Atrial Arrhythmias

Running title: *Herweg et al.; Atrio-atrial conduction in the transplanted heart*

Bengt Herweg, MD^{1,3}; Madhan Nellaiyappan, MBBS¹; Allan M. Welter-Frost, MD¹;
Thanh Tran, MPH^{1,3}; George Mabry, BS¹; Kathryn Weston, BS¹; Catalina Tobón, PhD⁴;
Javier Saiz, PhD⁵; Sami Noujaim, PhD^{1,2}; Mark W. Weston, MD^{1,3}



¹Department of Cardiovascular Sciences, ²Molecular Pharmacology and Physiology, University of South Florida Morsani College of Medicine; ³Tampa General Hospital, Tampa, Florida; ⁴Nanostructured Materials and Bio-modeling (MATBIOM), Universidad de Medellín, Medellín, Colombia; ⁵Centro de Investigación e Innovación en Bioingeniería (Ci²B), Universitat Politècnica de València, Valencia, Spain

Correspondence:

Bengt Herweg, MD, FACC, FHRS
USF Health South Tampa Center
2 Tampa General Circle
Tampa, FL 33606
Tel: (813) 259 0661
E-mail: bengt@usf.edu

Journal Subject Terms: Arrhythmias; Electrophysiology; Catheter Ablation and Implantable Cardioverter-Defibrillator; Transplantation

Abstract:

Background - The formation of recipient-to donor atrio-atrial connections (AAC) in patients after orthotopic heart transplantation (OHT) is poorly understood. We sought to investigate the mechanisms of atrial tachyarrhythmias after OHT, the role of AACs, and their relationship to the immunological match.

Methods - In a large series of OHT patients we performed a retrospective review of 42 patients who underwent catheter ablation for atrial arrhythmias. A realistic 3D computer model of human atria was used to study AAC conductivity.

Results - Patient age was 55 ± 15 years (71% male). 24/42 patients (57%) had bi-atrial anastomosis. An AAC was found in 9/42 patients (21%, right-sided in 5 patients with bi-atrial anastomosis, left-sided in 4 patients). The AAC became apparent at the time of the electrophysiology study 10.1 ± 7.6 years after OHT (range 0.3-22.2 years). Donor-specific antibodies (DSAB) were present in no patient with AAC, but were present in 69% of patients without AAC, $p=0.002$. In all patients with AAC, a recipient atrial tachycardia propagated via AAC to the donor atrium (4 patients presented with atrial fibrillation). Simulations showed AAC conduction requires an isthmus of ≥ 2 mm and is cycle length (CL) and location dependent. Patients without AAC ($n=13$) frequently presented with donor atrial arrhythmias, in 77% cavo-tricuspid isthmus (CTI) flutter was ablated. The procedural success was high, although, 12 patients (29%) required re-ablation.

Conclusions - AACs are found in 21% of OHT patients with atrial tachyarrhythmias and can manifest very early after OHT. Immune privilege characterized by the absence of DSAB may facilitate AAC formation. Propagation across an AAC is width, CL and location dependent. Patients with AAC present with focal atrial tachycardias or atrial fibrillation originating from the recipient atria; patients without most frequently present with CTI dependent atrial flutter. While multiple arrhythmias frequently require re-ablation, ablative therapy is highly effective.

Key words: atrial tachyarrhythmia; orthotopic heart transplant; arrhythmia (mechanisms); immunology; computer-based model

Nonstandard Abbreviations and Acronyms

AAC – atrio-atrial connections
 OHT – orthotopic heart transplantation
 CL – cycle length
 CTI – cavo-tricuspid isthmus
 PRA – panel reactive antibody
 DSAB – donor specific antibodies
 DF – dominant frequency
 AT – atrial tachycardia
 AF – atrial fibrillation
 AVNRT – atrio-ventricular nodal reentry tachycardia

Introduction

Atrial tachyarrhythmias following orthotopic heart transplantation (OHT) occur with a frequency of 5-44% early postoperatively (commonly with rejection), 7-9% late after transplantation,¹⁻⁴ and may be associated with increased mortality.⁵⁻⁶ Mechanisms involved include altered autonomic innervation, surgical trauma, rejection, inflammation, anastomosis type, and presence of recipient-to-donor atrio-atrial connections (AAC).¹⁻⁴ Mechanisms include abnormalities of impulse generation (focal atrial tachycardia) and propagation (reentry and conduction via AAC). While atrial flutter is frequent, atrial fibrillation is rare early postoperatively in stable OHT patients, likely due to surgical isolation of the recipient posterior left atrial segments, including pulmonary veins.²⁻⁴

The bi-atrial surgical technique involves incising the anterior portion of both donor atria and anastomosing them to the posterior wall of both recipient atria. With bi-caval technique, a small remnant of the recipient posterior left atrium between the pulmonary veins is anastomosed to the donor heart.

Formation of functional recipient-to-donor AACs after OHT is poorly understood.⁷⁻¹² We hypothesize cell-to-cell coupling between immunologically mismatched graft and host is jeopardized by local rejection and inflammation.

The aim of this clinical observational study was to investigate mechanisms of atrial tachyarrhythmias after OHT relevance of recipient-to-donor AACs, and their relationship to the immunological match. Computational modelling based on observed clinical electrophysiology was performed to understand mechanisms and requirements of electrical impulse propagation between recipient and donor cardiac tissue. We explored effects of AAC width, location, and cycle length (CL) of simulated atrial arrhythmias in a 3D model of the human atria with bi-caval and bi-atrial anastomosis.



Methods

The data that support findings of this study are available from the corresponding author upon reasonable request. Following Institutional Review Board approval, we retrospectively reviewed data from 1396 consecutive OHT recipients transplanted at Tampa General Hospital from 1988 until 2020, and 124 patients transplanted at other institutions. We identified 42 patients who underwent catheter ablation for atrial arrhythmias between 2005 and 2020 [34/42 patients (81%) were transplanted at our institution; 8/42 patients (19%) elsewhere]. At the time of first ablation in February 2005, 482 patients were being followed in our transplant clinic. Since then, 699 patients were transplanted. The incidence of catheter ablation in our cohort is estimated to be 42/1181 (3.6%).

The reviewed data spanning from pre-transplant work-up to most recent follow-up included electrocardiograms, rhythm strips, operative and electrophysiology reports. Standard

testing pre-/post-OHT included echocardiograms, cardiac catheterization with biopsies, and antibody panels [panel reactive antibody (PRA) and donor specific antibodies (DSAB)]. Data were compiled to determine type of arrhythmias evident, antibodies present, and evidence of vasculopathy and/or rejection.

Patients were started on medical therapy to control arrhythmias and, if refractory, offered ablation. Recurrent or new arrhythmias were treated medically, and if refractory, re-ablated.

Electrophysiology Study and Ablation

Three-dimensional electroanatomic mapping (Carto, Biosense Webster, Inc., Irvine, CA) of the right atrium was performed in all patients. Trans-septal catheterization and left atrial mapping was performed in 21 patients (50%). Recipient and donor atrial chambers were delineated using standard activation and voltage mapping techniques (differences in baseline rhythm frequently facilitated this process). Mapping density in general satisfied default Carto fill thresholds. Pacing and entrainment mapping delivered from recipient and donor atria with careful observation of the response in both chambers were used to diagnose AACs. In other instances, AACs were made apparent by arrhythmias propagating with a clear association, such as 2:1 or 1:1 conduction.

Arrhythmias occurred spontaneously or were induced by programmed stimulation off and on isoproterenol. In patients with clinical evidence of multiple arrhythmias, all were ablated if feasible. Ablation was performed with various catheter prototypes, more recently with irrigated force sensing catheters (7-French 3.5 mm tip SmartTouch ThermoCool, Biosense Webster, Inc., Irvine, CA). The earliest site of activation was targeted in focal atrial tachycardias while critical isthmus was targeted in macro-reentrant rhythm such as atrial flutter. Patients with evidence of atrial tachycardia or fibrillation driven by the recipient atrium underwent ablation of the AAC.

Computational simulations in a 3D model of human atria

The Courtemanche-Ramirez-Nattel-Kneller formalism was implemented to simulate human atrial action potential.^{13,14} This realistic 3D model of human atria included realistic fiber orientations, heterogeneity and anisotropy.¹⁵ Action potential propagation was modeled using the monodomain reaction–diffusion equation:

$$\frac{1}{S_v} \nabla \cdot (\mathbf{D} \nabla V_m) = C_m \frac{\partial V_m}{\partial t} + I_{ion} - I_{stim}$$

where V_m =membrane potential, S_v =surface-to-volume ratio, D =conductivity tensor, C_m =membrane capacitance, I_{ion} =total ionic membrane current and I_{stim} =stimulus current. Equations were numerically solved using EMOS software.¹⁶

We simulated bi-caval (Figures 1A and 1B) and bi-atrial (Figures 2A and 2B) anastomosis of 4 mm thickness and AAC isthmus widths of 1, 2, 4 and 6 mm. Left-sided AACs were located superiorly, inferiorly, septal or lateral (white arrows in Figures 1A and 1B). In bi-atrial anastomosis, right atrial AACs were located either superior- or inferior-laterally, or superior- or inferior-septally (white arrows in Figures 1A and 1B).

Normal electrophysiology (action potential duration ≈ 266 ms) was simulated in the donor atrium (green tissue). Mild remodeling was applied to the recipient atrium (orange) by simulating 10 nM of acetylcholine, shortening action potentials (≈ 156 ms) (Figures 1A, 1B, 2A and 2B). We applied a stimulation protocol, where S1 was sinus rhythm (CL of 1000 ms), S2 was an ectopic focus in the right superior pulmonary vein coupled at 300, 200 and 125 ms (red zones in Figures 1A and 2A).

Four electrograms 0.2 mm from the endocardial surface were computed to study AAC conduction. Electrogram 1 was located in the posterior left recipient atrium, 3 in the donor right atrial free wall, and 4 in the superior donor left atrium. Electrogram 2 was in the lateral donor

right atrium in bi-caval anastomosis (Figures 1A and 1B) and lateral recipient right atrium in bi-atrial anastomosis (Figures 2A and 2B). The extracellular potential (Φ_e) was computed using the following equation:

$$\phi_e(\vec{r}) = -K \iiint \vec{\nabla}' V_m(\vec{r}') \cdot \vec{\nabla}' \left[\frac{1}{|\vec{r}' - \vec{r}|} \right] dv$$

where K is a constant that includes the ratio of intracellular and extracellular conductivities, $\nabla' V_m$ is the spatial gradient of membrane potential, $\vec{r}' - \vec{r}$ is the distance from the source point (x, y, z) to the measuring point (x', y', z') and dv is the differential volume. Spectral analysis of the signals was performed using fast Fourier transform. The dominant frequency (DF) was calculated.

Statistical analysis

Continuous variables are expressed as mean \pm 1 standard deviation. Continuous variables were compared by two-tailed independent sample Student's t -test or Wilcoxon-rank-sum test (for non-normal distribution assessed by Shapiro-Wilk test). Categorical variables were compared by χ^2 or Fisher-exact test. A value of $p < 0.05$ indicated statistical significance. Statistical analysis was performed with SPSS (Version 25, IBM, Armonk, New York).

Results

Our cohort consisted of 42 OHT patients who underwent catheter ablation for supra-ventricular arrhythmias. The time from OHT to ablation was 10.1 ± 6.6 years (range 0.2-23.7 years). All patients had therapy refractory atrial arrhythmias or were medication intolerant (Table 1).

Bi-atrial anastomosis

Surgical reports and mapping defined a bi-atrial anastomosis in 24 patients (57%). From 1988 to 2002 the preferred surgical method was bi-atrial anastomosis (19/23 patients, 83%); since 2003,



bi-caval anastomosis (15/19 patients, 79%). In some patients with bi-atrial anastomosis, there was a small recipient atrial strip connecting both caval veins separated from the recipient left atrium. In others, we found a larger posterior right atrial segment that included the posterior septum connected to the recipient left atrial segment. Continuous electrical activation between right- and left-sided recipient atria was confirmed in 5/9 patients (55%) with bi-atrial anastomosis who underwent mapping and simultaneous recordings from both recipient atrial chambers. Right-sided recipient atrial rhythm was sinus or asystole in 16/24 patients (67%), atrial tachycardia (AT) in 6 patients (25%) and atrial fibrillation (AF) in 1 patient (4%).

Functional recipient-to-donor atrio-atrial connections

Of 42 patients, 9 (21%) demonstrated evidence of recipient-to-donor AACs. The AAC became apparent at the time of ablation, 0.3 years to 22.2 years after OHT (10.1±7.6 years). The AAC was located in the right atrium in 5 patients with bi-atrial anastomosis (4 superior, 1 lateral) and in the left atrium in 4 patients with bi-caval anastomosis (2 superior, 2 inferior). Left atrial mapping was performed in 21/42 patients (50%). Clinical characteristics of patients with and without AACs are summarized in Table 2. Patients are presented in three groups: 1. Documented AAC (n=9); 2. AAC ruled out by bi-atrial mapping (n=13); and 3. No clinical evidence of AAC by right atrial mapping only (n=20). The presenting arrhythmia in patients without AACs was more commonly reentrant atrial flutter. Those with AACs tended to present with focal AT or AF (Table 2). At time of ablation, we found recipient AT conducting via an AAC to the donor atrium in all patients with AAC (Table 3). Recipient focal AT was organized in 8/9 patients (CL was 272±50 ms, range 200-340 ms), disorganized paroxysmal AF in 1 patient, and originated from the pulmonary veins in 7/9 patients. In 2/9 patients with bi-atrial anastomosis, the tachycardia originated from a smaller right-sided recipient atrium electrically isolated from the

left sided recipient atrium. In 3/7 patients with pulmonary vein tachycardia, the AAC allowing donor atrial activation was right-sided. Reciprocating recipient-donor atrial reentry tachycardia is theoretically possible in presence of multiple functional AACs. Only single AACs were observed in this series (post-ablation conduction block between recipient and donor atrium).

Immunological studies

While all 9 patients with AACs did not have DSAB, 9/13 patients without AAC (69%) had DSAB, $p=0.002$ (Table 4). Vasculopathy tended to be insignificantly less frequent in patients with AACs, compared to patients without AAC ($p=0.07$). There were no significant differences in PRA, biopsy score, and peak biopsy grade comparing patients with/without AAC (Table 4).

Ablation of the recipient-to-donor atrio-atrial connection

In 8/9 patients, the AAC was targeted. At the ablation site, recipient and donor atrial potentials were recorded (temporal spacing ranged from 35 to 120 ms, in between frequently low amplitude fragmented activity). Ablation of the AAC required 1-3 radiofrequency energy applications to achieve complete conduction block (delivered radiofrequency applications 3.6 ± 1.5 including a few “insurance burns”). After ablation of the AAC, the recipient AT terminated in 2 patients and persisted in 6 patients. In one patient with paroxysmal AF and a massive left-sided recipient atrium and bi-caval anastomosis, we elected to perform an ostial pulmonary vein isolation procedure to eliminate the tachycardia preserving electrical activation of the large recipient left atrium (#9, Table 3). Figure 3 shows the activation map, CT scan, and intracardiac electrograms of patient #6 (Table 3), who had bi-caval anastomosis, displaying a left-sided inferior AAC, and a recipient AT (CL 320 ms) originating in the left upper pulmonary vein with 1:1 AAC conduction. Figure 4 shows the activation maps of three different tachycardias in patient #4 with bi-atrial anastomosis, superior right-sided recipient-to-donor AAC, and recipient AT (CL 300



ms) originating in the right upper pulmonary vein with a 1:1 AAC conduction. In Figure 5 we show patient #3 with bi-atrial anastomosis, a right-sided recipient AT (CL 280 ms) propagating 1:1 via a right-sided AAC.

Ablation of other arrhythmia mechanisms

The number of arrhythmias ablated per patient was 1.8 ± 0.9 (range 1-4). CTI dependent flutter was encountered in 27/42 OHT patients (64%, 25 counter-clock, 2 clockwise), and ablated in 2/9 patients with AACs (22%) compared to 10/13 OHT patients without AACs (77%), $p=0.01$ (Table 2). The CL of CTI dependent flutter was 247 ± 35 ms. The number of radiofrequency energy applications was 19 ± 11 to create bi-directional isthmus block. Bi-directional trans-isthmus delay was 178 ± 23 ms. Non-isthmus dependent atrial flutter occurred in 9/42 patients (21%, 4 right donor atrial scar flutters, 5 left donor mitral isthmus flutters). Focal atrial tachycardia originating from the donor atria was mapped and ablated in 13 patients (31%, 11 right sided foci, 2 left sided). There was no relationship to rejection or any immunologic parameter. Atrio-ventricular nodal reentry tachycardia (AVNRT) was ablated in 5/42 patients (12%) and not found in patients with AAC.

Long-term outcome of catheter ablation

The acute procedural success rate was high, though 12 patients (29%) required re-ablation (6 recurrences, 6 new arrhythmias, Tables 5/6). Multiple atrial arrhythmias were encountered in 21/42 patients (50%, 1.8 ± 0.9 per patient, range 1-4). CTI-dependent atrial flutter required re-ablation in 3 patients (all initially ablated with non-irrigated catheters). In one patient with bi-atrial anastomosis, bidirectional isthmus block could not be achieved in spite of re-ablation. In one patient with left-sided AAC, 2:1 conduction recovered requiring re-ablation. Symptom control was achieved in all patients, with 2 patients (5%) remaining on antiarrhythmic therapy

for multifocal atrial tachycardia. Implantation of a pacemaker was needed in two patients [loss of recipient sinus mechanism after ablation of the AAC in patient #5 (Table 3, Figure 6), AV block after a right-sided isthmus ablation due to compromised inputs into the AV node]. No procedure or arrhythmia related mortality occurred. The overall mortality during a follow-up of 5.0 ± 3.5 years was 40%.

3D computational modeling

Simulations of recipient atrial tachycardia showed conduction block at an AAC isthmus width of 1mm. An isthmus width ≥ 2 mm was necessary to allow conduction from the recipient to the donor atrium. An isthmus thickness of 4 mm was chosen to conduct further simulations. At a tachycardia CL of 300 ms, 1:1 conduction between recipient and donor atrium was observed for most AAC locations. However, 2:1 conduction occurred in half of the simulation trials with left sided septal AAC, and for bi-atrial anastomosis with superior and inferior lateral right sided AACs. Figures 1C and 2C show two episodes of focal tachycardia for bi-caval and bi-atrial anastomosis, respectively, with 1:1 conduction at a CL of 300 ms. There was recipient-to-donor propagation via the superior AAC (AAC– white arrows, ectopic focus – asterisk). The electrograms at defined atrial sites (Figures 1E and 2E) displayed single potentials, showing stable, regular activation during focal atrial tachycardia. There is a single narrow DF peak of 3.4 Hz in both, recipient and donor atrium reflecting regular activation and 1:1 AAC conduction.

At a tachycardia CL of 200 ms, 2:1 recipient-to-donor atrial conduction was observed (tachycardia CL > recipient atrial refractory period, and < donor atrial refractory period). Therefore, there was 2:1 recipient-to-donor conduction (DFs in donor atrium 1/2 DF in recipient atrium, single potentials at different atrial sites reflecting stable and regular atrial activation).

Fibrillatory conduction and re-entrant activity occurred when the tachycardia CL was 125 ms approaching recipient atrial refractoriness. In bi-caval anastomosis, reentrant activity was present only in the recipient left atrium, where 2:1 to 3:1 recipient-to-donor conduction patterns were observed. Figure 1D shows atrial fibrillation maintained by recipient left atrial reentrant activity, with 3:1 recipient-to-donor conduction via a superior AAC (curved arrows - wave front propagation; white arrows - AAC location; asterisk - ectopic focus location). Recipient atrial electrograms (Figure 1F) display CL and amplitude variations, indicating an unstable, irregular activation pattern characteristic of atrial fibrillation (multiple power spectral frequency peaks with a DF gradient: recipient atrium – 8.0 Hz, donor atrium – 2.8 Hz).

In bi-atrial anastomosis, reentrant activity in the recipient left atrium was observed in two cases: superior left atrial AAC and inferior right atrial AAC. In six additional simulations of various AAC locations, reentrant activity occurred in both recipient atria. Reentrant activity was intermittent, and more stable in the left compared to the right atrium (1.3:1 to 4:1 recipient-to-donor conduction). Figure 2D shows an episode of atrial fibrillation maintained by re-entrant activity in both recipient atria (curved arrows – reentrant wave front propagation). There was right superior recipient-to-donor AAC conduction (white arrow) with variable 3.6:1 conduction block. The recipient and donor atrial electrograms (Figure 2F) display CL and amplitude variations and unstable, irregular atrial activation (multiple power spectral frequency peaks with a DF gradient: left and right recipient atrium - 8.0 Hz, left and right donor atrium - 2.2 Hz). The corresponding video clips for Figures 1C&D and 2C&D can be viewed online.

Discussion

This large cohort of OHT patients who underwent catheter ablation allowed us to investigate the recipient-to-donor AAC phenomenon in detail. Functional AACs are found in at least 21% of OHT patients presenting with atrial tachyarrhythmias. Their prevalence in asymptomatic OHT patients is unknown. AACs can be manifest early after OHT. Immune privilege characterized by the absence of DSAB may facilitate the formation of AACs. Propagation across an AAC appears to be width, CL and location dependent. Patients with AACs frequently present with focal recipient atrial tachycardias or atrial fibrillation, propagating to the donor atria via the AAC. Patients without AAC present with donor atrial arrhythmias, most commonly CTI dependent atrial flutter.



Atrial arrhythmias occur in 18-50% of OHT patients and appear to be more prevalent than ventricular arrhythmias.^{1,5,17} Some studies have shown an association with rejection^{2,17,18,19} while others, in cyclosporin treated patients, have not.^{1,20}

Recipient-to-donor AAC after OHT was first suspected in 1983, based on electrocardiographic recordings by Bexton et al.⁷ and confirmed by invasive studies by Anselme et al. in 1994.⁸ Rate-dependent bidirectional block was demonstrated and a potential relationship to arrhythmias emphasized. Rothman and colleagues in 1995 first described a clinical recipient-to-donor atrial tachycardia treated by radiofrequency ablation of the AAC in the lateral right atrial anastomosis.⁹ A subsequent study attempted to determine the frequency of recipient-to-donor conduction in asymptomatic patients with OHT. A study of 50 patients >5 years after OHT analyzed electrocardiographic changes in P wave morphology during exercise (and atrial premature beats with various coupling intervals), demonstrating potential AAC in 5 patients (10%).¹¹ The true incidence of AACs in asymptomatic OHT patients remains unknown.

Nof et al. reported the frequency of AACs in OHT patients with supra-ventricular arrhythmias undergoing ablative therapy to be 4/15 (27%, 3 right-sided, 1 left sided).²¹ Recipient tachycardias propagating to the donor atria were found in 3/4 patients. Elsik et al. demonstrated AACs in 2/16 (13%, both right sided).²² In a recent report by Mouhoub et al. recipient-to-donor AACs were found in 6/30 patients (20%) undergoing ablation. Surprisingly, no patients had clinical arrhythmias related to AAC conduction and, therefore, no ablation was performed (AAC location not specified).²³ The frequency of AACs in our cohort (21%) is consistent with these observations, however, in all 9 patients propagation of a recipient tachycardia to the donor atrium was demonstrated.

Three possible mechanisms of electrical impulse propagation across suture lines have been considered: mechanical coupling, electrotonic field effect, and direct electrical conduction. Mechanical coupling is unlikely considering the observed rate-dependent changes in conduction and the predictable ablation success along the suture line.⁹⁻¹² Another possible mechanism is electrotonic field effect which does not require direct conduction across the suture line. Ionic currents provoke depolarization in nearby myocardium across an intervening region of impaired conductivity (i.e., scar) without the passage of an action potential.²⁴ The most likely explanation appears to be direct electrical conduction across the suture line by a bridge of excitable myocardium crossing the atrio-atrial anastomosis. Pressure and alignment related to suturing may play an important role.¹² Denfield and colleagues described viable myocardium within most fibrous scars 5 months after ventriculotomies and atriotomies in dogs.²⁵ Razzouk and coworkers described conduction across an atrio-ventricular anastomosis following surgery for tricuspid atresia, creating a surgical Wolff-Parkinson-White syndrome (which had failed in prior animal experimental models).²⁶ It is unclear if cell-to-cell conduction is mediated by cardiac myocytes

with or without gap junctional conduction or other cell types. In sex-mismatched OHT recipients, newly formed cardiomyocytes were found that had intercellular connections and appeared to be electrically coupled with surrounding cardiomyocytes via gap junctions. This finding suggested that under special circumstances the heart can regenerate.²⁷

Denervation is an immediate consequence of OHT. Re-innervation can occur over time, implying an extension of recipient cells into the donor milieu.²⁸ By looking at sex-mismatched cardiac allografts and the presence of Y-chromosome cells as identified by in situ hybridization, it has been demonstrated that cardiac myocytes as well as endothelial cells, smooth muscle cells and Schwann cells can all develop within donor tissue.²⁷⁻³¹ This chimerism seen amongst OHT patients can develop as soon as 4 days and up to 1 month after OHT. In our cohort, the AAC became apparent as early as 0.3 years and as late as 22.2 years after ablation (10.2 ± 7.6 years). The duration of its existence prior to ablation remains uncertain. Chimeric tissue provides a possible explanation for the formation of AACs.

A variety of immune regulatory cells are vital to allograft survival by mitigating and regulating the inflammatory response produced by effector cells, thus, playing a role in the preservation of transplanted organs. CD4 positive T-regulatory cells can prevent rejection.³²⁻³³ Both, the host and allograft tissue can stimulate the production of these T-regulatory cells, thereby favoring survival. Additional immune cells known to impact allograft survival include regulatory B cells, macrophages, immature dendritic cells, myeloid-derived suppressor cells and mesenchymal stromal cells.³⁴⁻³⁶ The regulatory immune cell's impact on the effector cells in conjunction with immunosuppressive therapy promote graft longevity.

A key determinant to ensure graft survival and successful transplantation involves allosensitization, the presence of antibodies to human leukocyte antigens (HLA) and non-human

leukocyte antigens.^{37,38} Incompatibility among tissue types may be present at baseline or can be the result of antigen exposure. The development of DSAB are a serious threat as they are associated with increased morbidity and mortality post-transplant. The absence of allosensitization can lead to recipient stem cell myocyte regeneration. In this study, 25/42 (59%) had no evidence of DSAB. The 9 patients with an AAC did not have any evidence of DSAB or rejection. The lack of DSAB indicates a greater degree of histocompatibility and closer immunologically match.

Observations during computer modeling

Our simulations showed propagation across an AAC requires an isthmus width of at least 2 mm and is CL dependent. Arrhythmias with slower CLs, such as focal recipient atrial tachycardia, conduct through the isthmus in a 1:1 or 2:1 pattern. More rapid tachyarrhythmias, such as atrial fibrillation, develop less stable conduction patterns compared to atrial tachycardia. As a result, DF gradients form between recipient and donor atrial tissue. Conductivity appears to be location dependent, possibly related to differences in fiber alignment at the site of the anastomosis.

Donor atrial arrhythmias

In patients without AAC, arrhythmias originate from the donor atria. Donor arrhythmias include reentrant atrial flutter, focal atrial tachycardia or AVNRT. CTI-dependent atrial flutter was the most common donor atrial arrhythmia (64% of patients), present in 77% of patients without AAC versus 22% of patients with AACs ($p=0.01$, Table 2). Non-CTI dependent donor atrial flutter was found in 21% of patients (right-sided, scar dependent in 4 patients; left-sided mitral annular, in 5 patients). Donor focal atrial tachycardia was ablated in 31% of patients (11 right sided foci, 2 left sided). In 5 patients (12%), typical AVNRT was ablated.

Long-term outcome after catheter ablation

The acute procedural success rate was high, with symptom control achieved in all patients (5% remained on antiarrhythmic therapy). Of 12 patients requiring re-ablation, there were 6 arrhythmia recurrences and 6 new arrhythmias. Multiple atrial arrhythmias were frequently encountered. CTI dependent atrial flutter required re-ablation in 3/27 patients (11%). In one patient with a left sided AAC, 2:1 conduction recovered requiring re-ablation. Pacemaker implantations were required post-ablation in two patients. While no procedure or arrhythmia related mortality occurred, mortality during follow-up of 5.0 ± 3.5 years was 40%, comparable to previously published reports.²¹⁻²³

Conclusion

The development of arrhythmias following OHT is influenced by donor and host predispositions, surgical techniques, and presence/absence of recipient-to-donor AACs. Functional AACs are found in 21% of OHT patients presenting with atrial tachyarrhythmias. Their prevalence in asymptomatic patients after OHT is unknown. AACs can be manifest early after OHT. Immune privilege, characterized by the absence of DSAB, may facilitate AAC development.

Computational modeling showed propagation across an AAC requires an isthmus width of ≥ 2 mm and conduction is CL and location dependent. Patients with AAC present with recipient focal atrial tachycardias or atrial fibrillation, propagating to the donor atria via the AAC.

Patients without AAC present with donor atrial arrhythmias, most commonly CTI dependent atrial flutter. Multiple arrhythmias are frequently encountered, resulting in 29% re-ablation rate.

The long-term outcome after catheter ablation is excellent. Further studies in larger OHT patient populations with and without atrial arrhythmias are needed to delineate the exact mechanism of recipient-to-donor AACs.



Limitations

Clinical observational study

While this is a large cohort of OHT patients undergoing ablative therapy, it remains a retrospective observational study. Only 50% of patients underwent left atrial mapping.

Determination of the frequency of functional AAC, including in asymptomatic patients, requires prospective studies.

Computational modeling

Our simulation results were obtained using a virtual atrial model which formulated excellent anatomical and morphological details (i.e. electrophysiology, anatomy, fiber direction, anisotropy and heterogeneity). The simulation was limited in its ability to incorporate fibrosis.

Considering functional reentry and rotors have been widely reported as maintenance mechanisms of atrial arrhythmias, future works must include structural remodeling.

Sources of Funding: Supported in part by National Institutes of Health grants R21HL138064, and R01HL129136 to SN. This work was partially supported by the Direcció General de Política Científica de la Generalitat Valenciana (PROMETEU2020/043).

Disclosures: None

Supplemental Material:

Video I-IV

References:

1. Jacquet L, Ziady G, Stein K, Griffith B, Armitage J, Hardesty R, Kormos R. Cardiac rhythm disturbances early after orthotopic heart transplantation: prevalence and clinical importance of the observed abnormalities. *J Am Coll Cardiol.* 1990;16:832–7.

2. Vaseghi M, Boyle NG, Kedia R, Patel JK, Cesario DA, Wiener I, Kobashigawa JA, Shivkumar K. Supraventricular tachycardia after orthotopic cardiac transplantation. *J Am Coll Cardiol*. 2008;51:2241-9.
3. Cohn WE, Gregoric ID, Radovancevic B, Wolf RK, Frazier OH. Atrial fibrillation after cardiac transplantation: Experience in 498 consecutive cases. *Ann Thorac Surg*. 2008;85:56-58.
4. Khan M, Kalahasti V, Rajagopal V, Khaykin Y, Wazni O, Almahameed S, Zuzek R, Shah T, Lakkireddy D, Saliba W, et al. Incidence of atrial fibrillation in heart transplant patients: long-term follow-up. *J Cardiovasc Electrophysiol*. 2006;17:827-31.
5. Pavri BB, O'Nunain SS, Newell JB, Ruskin JN, William G. Prevalence and prognostic significance of atrial arrhythmias after orthotopic cardiac transplantation. *J Am Coll Cardiol*. 1995;25:1673-1680.
6. Ahmari SA, Bunch TJ, Chandra A, Chandra V, Ujino K, Daly RC, Kushwaha SS, Edwards BS, Maalouf YF, Seward JB, et al. Prevalence, pathophysiology, and clinical significance of post-heart transplant atrial fibrillation and atrial flutter. *J Heart Lung Transplant*. 2006;25:53-60.
7. Bexton RS, Hellestrand KJ, Cory-Pearce R, Spurrell RA, English TA, Camm AJ. Unusual atrial potentials in a cardiac transplant recipient. Possible synchronization between donor and recipient atria. *J Electrocardiol*. 1983;16:313-322.
8. Anselme F, Saoudi N, Redonnet M, Letac B. Atrioatrial conduction after orthotopic heart transplantation. *J Am Coll Cardiol*. 1994;24:185-9.
9. Rothman SA, Miller JM, Hsia HH, Buxton AE. Radiofrequency ablation of a supraventricular tachycardia due to interatrial conduction from the recipient to donor atria in an orthotopic heart transplant recipient. *J Cardiovasc Electrophysiol*. 1995;6:544-50.
10. Saoudi N, Redonnet M, Anselme F, Poty H, Cribier A. Catheter ablation of atrioatrial conduction as a cure for atrial arrhythmia after orthotopic heart transplantation. *J Am Coll Cardiol*. 1998;32:1048-55.
11. Lefroy DC, Fang JC, Stevenson LW, Hartley LH, Friedman PL, Stevenson WG. Recipient-to-donor atrioatrial conduction after orthotopic heart transplantation: Surface electrocardiographic features and estimated prevalence. *Am J Cardiol*. 1998;82:444-450.
12. Birnie D, Green MS, Veinot JP, Tang AS, Davies RA. Interatrial conduction of atrial tachycardia in heart transplant recipients: potential pathophysiology. *J Heart Lung Transplant*. 2000;19:1007-10.
13. Courtemanche M, Ramirez RJ, Nattel S. Ionic mechanisms underlying human atrial action potential properties: insights from a mathematical model. *Am J Physiol*. 1998;275:H301-H321.



14. Kneller J, Zou R, Vigmond EJ, Wang Z, Leon J, Nattel S. Cholinergic atrial fibrillation in a computer model of a two-dimensional sheet of canine atrial cells with realistic ionic properties. *Circ Res*. 2002;90:E73–87.
15. Tobón C, Ruiz-Villa C, Heidenreich E, Romero L, Hornero F, Saiz J. A Three-Dimensional Human Atrial Model with Fiber Orientation. Electrograms and Arrhythmic Activation Patterns Relationship. *PLoS One*. 2013;8:e50883.
16. Heidenreich EA, Ferrero JM, Doblaré M, Rodríguez JF. Adaptive macro finite elements for the numerical solution of monodomain equations in cardiac electrophysiology. *Ann Biomed Eng*. 2010;38:2331–2345.
17. Scott CD, Dark JH, McComb JM. Arrhythmias after cardiac transplantation. *Am J Cardiol*. 1992;70:1061–3.
18. Berke DK, Graham AF, Schroeder JS, Harrison DC. Arrhythmias in the denervated transplanted human heart. *Circulation*. 1973;47:112–15.
19. Caves PK, Stinson EB, Billingham ME, Shumway NE. Serial transvenous biopsy of the transplanted human heart. *Lancet*. 1974;i:821–6.
20. Little RE, Kay N, Epstein AE, Plumb VJ, Bourge RC, Neves J, Jirkin JK. Arrhythmias after orthotopic cardiac transplantation. *Circulation*. 1989;80(Suppl III):140–6.
21. Nof E, Stevenson WG, Epstein LM, Tedrow UB, Koplan BA. Catheter ablation of atrial arrhythmias after cardiac transplantation: Findings at EP study utility of 3-D mapping and outcomes. *J Cardiovasc Electrophysiol*. 2013;24: 498-502.
22. Elsik M, The A, Ling LH, Virdee M, Parameshwar J, Fynn SP, Kistler PM. Supraventricular arrhythmias late after orthotopic cardiac transplantation: electrocardiographic and electrophysiological characterization and radiofrequency ablation. *EP Europace*. 2012;14:1498–1505.
23. Mouhoub Y, Laredo M, Varnous S, Leprince P, Waintraub X, Gandjbakhch E, Hebert JL, Frank R, Maupain C, Pavie A, et al. Catheter ablation of organized atrial arrhythmias in orthotopic heart transplantation. *J Heart Lung Transplant*. 2018;37:232-239.
24. Jalife J, Moe GK. A biological model of parasystole. *Am J Cardiol*. 1979;43:761–72.
25. Denfield SW, Kearney DL, Michael L, Gittenberger-de-Groot A, Garson A. Developmental differences in canine cardiac surgical scars. *Am Heart J*. 1993;126:382–389.
26. Razzouk AJ, Gow R, Finley J, Murphy D, Williams W. Surgically created Wolff-Parkinson-White syndrome after Fontan operation. *Ann Thorac Surg*. 1992;54:974–977.

27. Muller P, Pfeiffer P, Koglin J, Schafers HJ, Seeland U, Janzen I, Urbschat S, Bohm M. Cardiomyocytes of noncardiac origin in myocardial biopsies of human transplanted hearts. *Circulation*. 2002;106:31-35.
28. Minami E, Laflamme MA, Saffitz JE, Murry CE. Extracardiac progenitor cells repopulate most major cell types in the transplanted human heart. *Circulation*. 2005;112:2951-2958.
29. Quaini F, Urbanek K, Beltrami AP, Finato N, Beltrami CA, Nadal-Ginard B, Kajstura J, Leri A, Anversa P. Chimerism of the transplanted heart. *N Engl J Med*. 2002;346:5-15.
30. Glaser R, Lu MM, Narula N, Epstein JA. Smooth muscle cells, but not myocytes, of host origin in transplanted human hearts. *Circulation*. 2002;106:17-19.
31. Simer D, Wang S, Deb A, Holmes D, McGregor C, Frantz R, Kushwaha SS, Caplice NM. Endothelial progenitor cells are decreased in blood of cardiac allograft patients with vasculopathy and endothelial cells of non-cardiac origin are enriched in transplant atherosclerosis. *Circulation*. 2003;108:143-149.
32. Issa F, Wood KJ. CD4+ regulatory T cells in solid organ transplantation. *Curr Opin Organ Transplant*. 2010;15:757-764.
33. Kingsley CT, Karim M, Bushell AR, Wood KJ. CD25+CD4+ regulatory T cells prevent graft rejection: CTLA-4- and IL-10-dependent immunoregulation of alloresponses. *J Immunol*. 2002;168:1080-1086.
34. Podesta MA, Remuzzi G, Casiraghi F. Mesenchymal Stromal Cells for Transplant Tolerance. *Front Immunol*. 2019;10:1287.
35. Wood KJ, Bushell A, Hester J. Regulatory Immune Cells in Transplantation. *Nat Rev Immunol*. 2012;12:417-430.
36. Hu C, Wu Z, Li L. Mesenchymal stromal cells promote liver regeneration through regulation of immune cells. *Intl Journal Biological Sciences*. 2020;16:893-903.
37. Valenzuela NM, Reed EF. Antibodies in Transplantation: The Effects of HLA and Non-HLA Antibody Binding and Mechanisms of Injury. *Methods Mol Biol* 2013;1034:41-70.
38. Tambur AR, Pamboukian SV, Costanzo MR, Herrera ND, Dunlap S, Montpetit M, Heroux A. The presence of HLA-directed antibodies after heart transplantation is associated with poor allograft outcome. *Transplantation* 2005;80:1019-1025.

Table 1. Baseline Characteristics

Baseline Characteristics	n = 42
Age (years)	55±15 (22-79)
Male	30 (71%)
Etiology of cardiomyopathy	
Ischemic	12 (29%)
Non-ischemic	30 (71%)
Year of orthotopic heart transplantation	1988-2017
Bi-atrial anastomosis	24 (57%)
Time from transplant to ablation (years)	10.1±6.6 (range 0.2-23.7)
Transplant vasculopathy	14 (33%)
Donor specific antibodies	17 (40%)
Ejection fraction at time of ablation (%)	54±11



Circulation: Arrhythmia and Electrophysiology

Table 2. Clinical Characteristics of Patients With and Without Recipient-to-Donor Atrio-Atrial Connections

	AAC* (n=9) (LA mapping performed in 8/9 patients)	No AAC* (n=13) (LA mapping performed)	No AAC* evident (n=20) (LA mapping not performed)	p
Age (years)	59±13	56±15	52±16	ns
Male gender	5 (55%)	10 (77%)	15 (75%)	ns
Bi-atrial anastomosis	5 (55%)	6 (46%)	13 (65%)	ns
Time from transplant to ablation (years)	10.2±7.6	10.9±7.2	9.6±5.9	ns
Presenting arrhythmia				
Atrial flutter	1 (11%)	9 (69%)	11 (55%)	0.007 [#] /0.03 ^{**}
Focal atrial tachycardia	7 (78%)	5 (38%)	7 (35%)	0.07 [#] /0.03 ^{**}
Atrial fibrillation	4 (44%)	1 (8%)	0	0.04 [#] /0.02 ^{**}
Short RP tachycardia	0	0	4 (20%)	ns
Ablated arrhythmia				
CTI dependent flutter	2 (22%)	10 (77%)	15 (75%)	0.01 [#] /0.007 ^{**}
Non-CTI dependent flutter	2 (22%)	5 (38%)	2 (10%)	ns
AVNRT [§]	0	1 (8%)	4 (20%)	ns
Focal donor AT [‡]	3 (33%)	4 (31%)	6 (30%)	ns
Focal recipient AT [‡] /AF [†] conducting via AAC*	9 (100%)	0	0	0.00001 ^{###}
Number of procedures (median/IQR)	1.0/1.0	1.0/1.0	1.0/1.0	ns
Arrhythmias ablated (median/IQR)	2.0/2.0	2.0/1.0	1.5/1.0	ns

*AAC=recipient-to-donor atrio-atrial connection, †AF=atrial fibrillation, ‡AT=atrial tachycardia, §AVNRT=atrio-ventricular nodal reentry tachycardia, |LA=left atrium, #comparing patients with AAC to no AAC, **comparing patients with AAC to no AAC evident

Table 3. Characteristics of Atrial Arrhythmias in Patients With Recipient-to-Donor Atrio-Atrial Connections

#	Anastomosis	Location of AAC*	Tachycardia Origin	CL [†]	Conduction via AAC	AV nodal Conduction
1	Bi-atrial	Superior RA [‡]	PVs	285	2:1	1:1
2	Bi-atrial	Superior RA	PVs	200	2:1	1:1
3	Bi-atrial	Lateral RA	Recipient RA	280	1:1	Irregular
4	Bi-atrial	Superior RA	RU [#] PV	300	1:1	Irregular
5	Bi-atrial	Superior RA	Recipient RA	340	1:1	2:1
6	Bi-caval	Inferior LA [§]	LU ^{**} PV	320	1:1	2:1
7	Bi-caval	Inferior LA	PVs	213	1:1	Irregular
8	Bi-caval	Superior LA	LU PV	240	2:1	1:1
9	Bi-caval	Superior LA	All PVs	PAF ^{††}	irregular	1:1

*AAC=recipient-to-donor atrio-atrial connection, [†]CL=cycle length, [‡]RA=right atrium, [§]LA=left atrium, [|]PV=pulmonary vein, [#]RU=right upper, ^{**}LU=left upper, ^{††}PAF=paroxysmal atrial fibrillation

**Table 4.** Immunology in Patients With and Without Recipient-to-Donor Atrio-Atrial Connections

	AAC* (n=9) (LA [‡] mapping performed in 8/9 patients)	No AAC* (n=13) (LA [‡] mapping performed)	No AAC* evident (n=20) (LA [‡] mapping not performed)	P
DSAB [†] present	0 (0%)	9 (69%)	8 (40%)	0.002
Vasculopathy (+)	2 (22%)	8 (62%)	4 (20%)	0.07
PRA [§] at transplantation (+)	1/8 (12%)	3/12 (25%)	4/16 (25%)	ns
Peak PRA [§] at transplantation (continuous) (median/IQR)	0.00/1.00	0.00/1.00	0.00/6.00	ns
Data missing	1 (11%)	1 (8%)	4 (20%)	(0.15)
Peak biopsy grade (1 st year)	1.00/2.00	1.00/2.00	2.00/3.00	ns
Peak biopsy grade (>1 year)	1.00/1.00	1.00/2.00	1.00/1.00	ns
Biopsy Score (median/IQR)	0.23/0.13	0.12/0.33	0.19/0.44	ns

*AAC=recipient-to-donor atrio-atrial connection, [†]DSAB=donor specific antibodies, [‡]LA=left atrium, [§]PRA=panel reactive antigen, [|] comparing patients with AAC to no AAC

Table 5. Catheter Ablation – Outcome

Outcome	n=42
Procedure time (min)	189±104
Fluoroscopy time (min)	22±18
Follow up after ablation (years)	5.0±3.5 (range 0.1-12.5) (Median 3.1, IQR* 0.1-6.7) Lost to follow up 3/42 (7%)
Procedures per patient	1.4 ± 0.6 (range 1-3)
Arrhythmias ablated per patient	1.8 ± 0.9 (range 1-4)
Patients requiring re-ablation	12 (29%)
Novel arrhythmia	6
Recurrence of prior arrhythmia	6
Time to recurrent arrhythmia (years)	1.2±2.3
Permanent pacemaker post-procedure	2 (5%)
Patients on anti-arrhythmic therapy	2 (5%)
Deaths during follow-up	17 (40%)
Time from ablation until death (years)	3.6±2.5
Death associated with ablation procedure	0

*IQR=interquartile range



Table 6. Re-ablation Procedures

#	Procedure 1	Time to Re-ablation (days)	Procedure 2	Time to Re-ablation (days)	Procedure 3	AAC* (yes/no)
1	CTI [†] flutter	164	Mitral isthmus flutter	-	-	no
2	Focal right atrial donor tachycardia	18	CTI [†] flutter	-	-	no
3	CTI [†] flutter	28	CTI [†] flutter	-	-	no
4	CTI [†] flutter	223	Mitral isthmus flutter	-	-	no
5	CTI [†] flutter	877	CTI [†] flutter	-	-	no
6	Focal right atrial donor tachycardia	63	Multifocal right atrial donor tachycardia	-	-	no
7	CTI [†] flutter Right non-CTI flutter	188	Right non-CTI flutter	-	-	no
8	CTI [†] flutter	2926	Focal right atrial donor tachycardia	-	-	no
9	Left atrial recipient tachycardia (via left AAC)	22	Left atrial recipient tachycardia (via left AAC*)	-	-	yes
10	CTI [†] flutter, multifocal right atrial donor tachycardia	170	Left atrial recipient tachycardia (via left AAC*)	-	-	yes
11	CTI [†] flutter	7	CTI [†] flutter	18	Multifocal right atrial donor tachycardia	no
12	Right atrial recipient tachycardia (via right AAC*)	445	Focal right atrial donor tachycardia	6	Multifocal right atrial donor tachycardia	yes

*AAC=atrio-atrial connection, †CTI=cavo-tricuspid isthmus dependent

Circulation: Arrhythmia and Electrophysiology

Figure Legends:

Figure 1. 3D computational modeling in bi-caval anastomosis (panels **A** and **B**). White arrows indicate the locations of the atrio-atrial connection (AAC) scenarios simulated. The numbers indicate the location of the calculated electrograms. **C.** Voltage snapshots of a recipient focal right superior pulmonary vein tachycardia (CL= 300 ms, white asterisk) propagating via a left superior AAC (4 mm thickness, white arrow). **E.** Electrograms recorded in the locations 1-4 and their respective power spectra. **D.** Recipient atrial fibrillation (CL= 125ms) maintained by reentry (curved arrows). **F.** Electrograms recorded from locations 1-4 and their respective power spectra.



Figure 2. 3D computational modeling in bi-atrial anastomosis (panels **A** and **B**). White arrows indicate the locations of the atrio-atrial connection (AAC) scenarios simulated. The numbers indicate the location of the calculated electrograms. **C.** Voltage snapshots of a recipient focal right superior pulmonary vein tachycardia (CL= 300 ms, white asterisk) with a superior right atrial AAC (4 mm thickness, white arrow). **E.** Electrograms recorded from locations 1-4 and their respective power spectra. **D.** Atrial fibrillation (CL= 125ms) maintained by recipient bi-atrial reentry (curved arrows). **F.** Electrograms recorded from locations 1-4 and their respective power spectra.

Figure 3. Endocardial activation map, CT scan, and intracardiac electrograms in a patient with left sided recipient-to-donor atrio-atrial connection (AAC) (patient #6). **A.** Left atrial tachycardia (AT) originating from the posterior wall of the recipient atrium: AAC in the infero-posterior

aspect of the anastomosis (arrow). The CT scan (left panel) demonstrates a tissue bridge of 3mm width between recipient and donor atrium. **B.** Radiofrequency energy delivery at the AAC resulted in immediate isolation of the recipient atrium with persistent recipient AT, but donor sinus rhythm. The ablation catheter recorded near field recipient atrial signals and far field donor atrial signals.

Figure 4. Endocardial activation maps of three tachycardias in a patient with right sided recipient-to-donor atrio-atrial connection (AAC) (patient #4). **A.** AT originating from the septal aspect of the left sided recipient atrium. Recipient-to-donor conduction via a right-sided AAC with late activation of the left-sided donor atrium. The tachycardia was terminated by ablation at the site of earliest activation. The AAC was ablated, resulting in isolation of the recipient atria. **B.** Left-sided donor atrial flutter revolved around the mitral annulus. Ablation in the area of the mitral isthmus connecting the valve to the anastomosis line terminated this flutter. Additional lesions were delivered inside the coronary sinus, resulting in bidirectional block. Panel **C.** An AT from the septal donor left atrium terminated by ablation at the site of earliest activation.

Figure 5. Bi-atrial anastomosis: Recipient right atrial tachycardia propagating via right-sided atrio-atrial connection (AAC) to the donor atrium (patient #3). Endocardial voltage map of the recipient atria (panel **A**, red) and the donor atria (panel **B**, blue). Endocardial activation map (panel **C**) with the corresponding voltage map (panel **D**) shows earliest activation in the postero-lateral recipient atrium. The Pentaray electrograms displayed on the left (dashed arrows) show recipient and donor atrial signals with fragmented activity. Ablation of the AAC (blue lesion) terminated the tachycardia in the donor atrium.

Figure 6. Competing sinus mechanisms from recipient and donor right atrium (patient #5). On the left side of the tracing there is recipient-to-donor atrio-atrial conduction (AAC), with a gradual takeover of the donor atrial sinus mechanism associated with a change in P-wave morphology. After AAC ablation, the patient lacked any donor sinus mechanism requiring pacemaker therapy.



Circulation: Arrhythmia and Electrophysiology

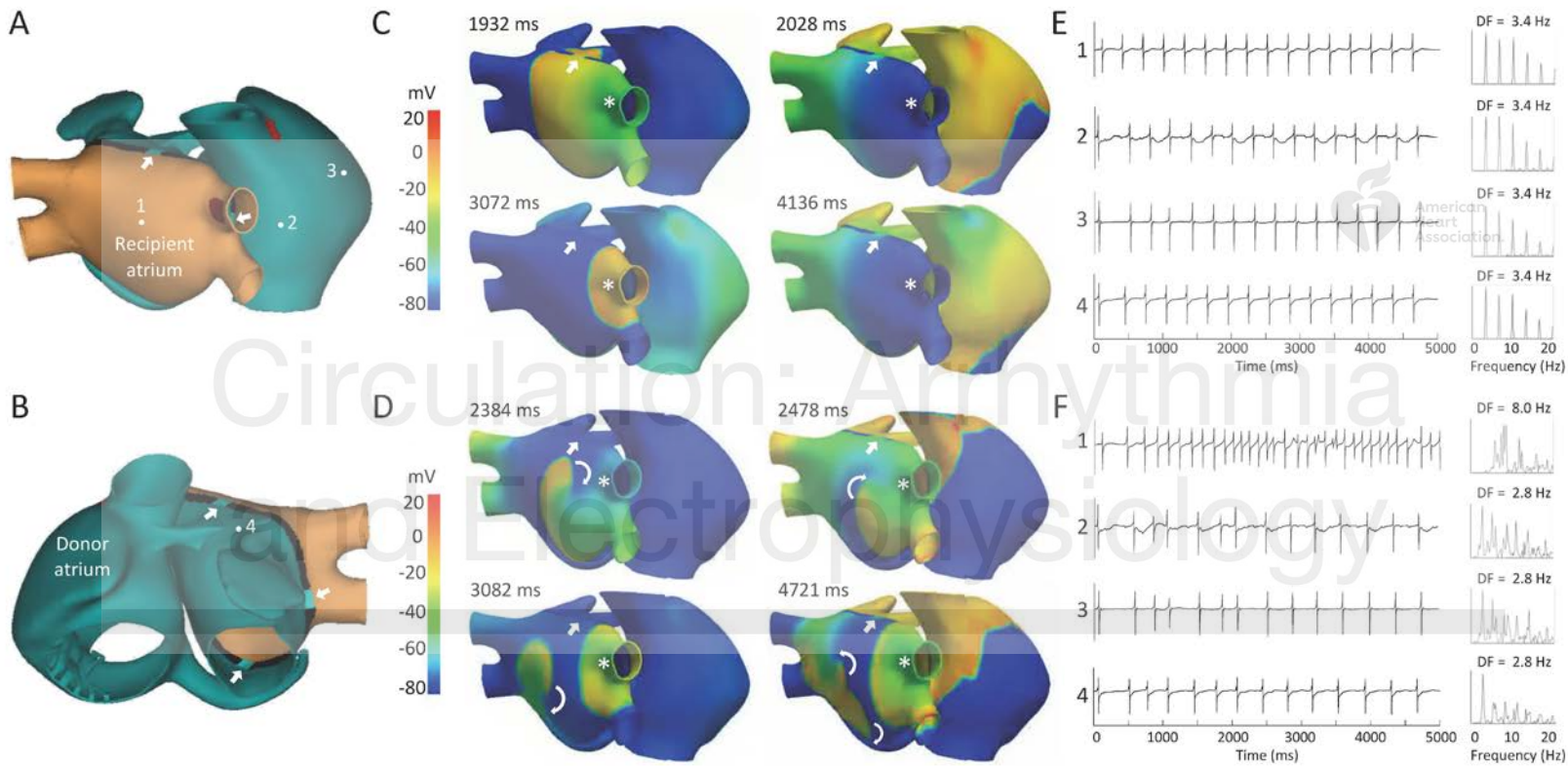
What Is Known?

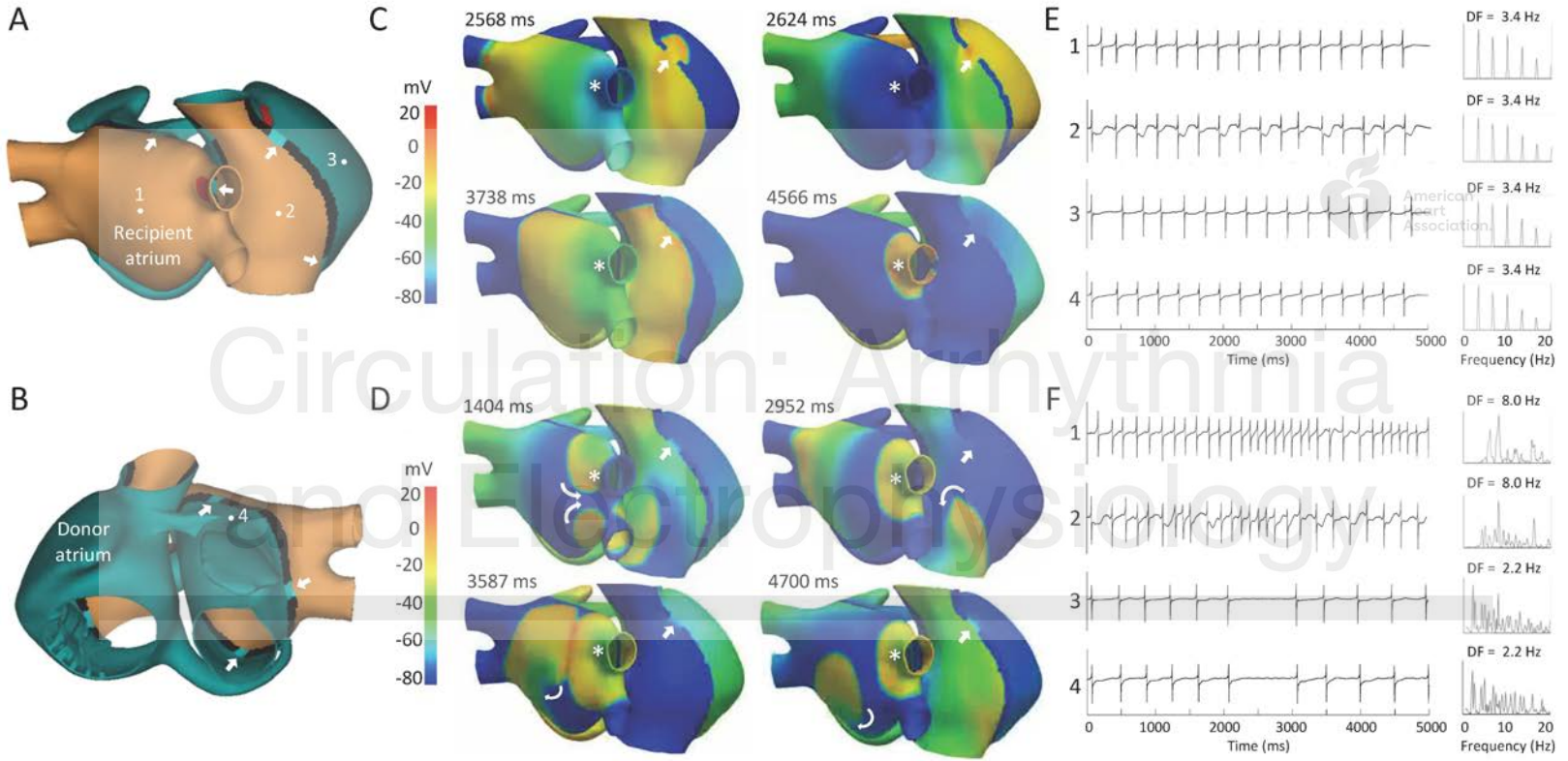
- Atrial tachyarrhythmias following orthotopic heart transplantation occur with a frequency of 5-44% early postoperatively, 7-9% late after transplantation, and may be associated with increased mortality.
- While atrial flutter is frequent, atrial fibrillation is rare early postoperatively in stable heart transplant patients, likely due to surgical isolation of the recipient posterior left atrial segments, including pulmonary veins.
- Recipient-to-donor atrio-atrial connections have been reported after heart transplantation, but their development is poorly understood.

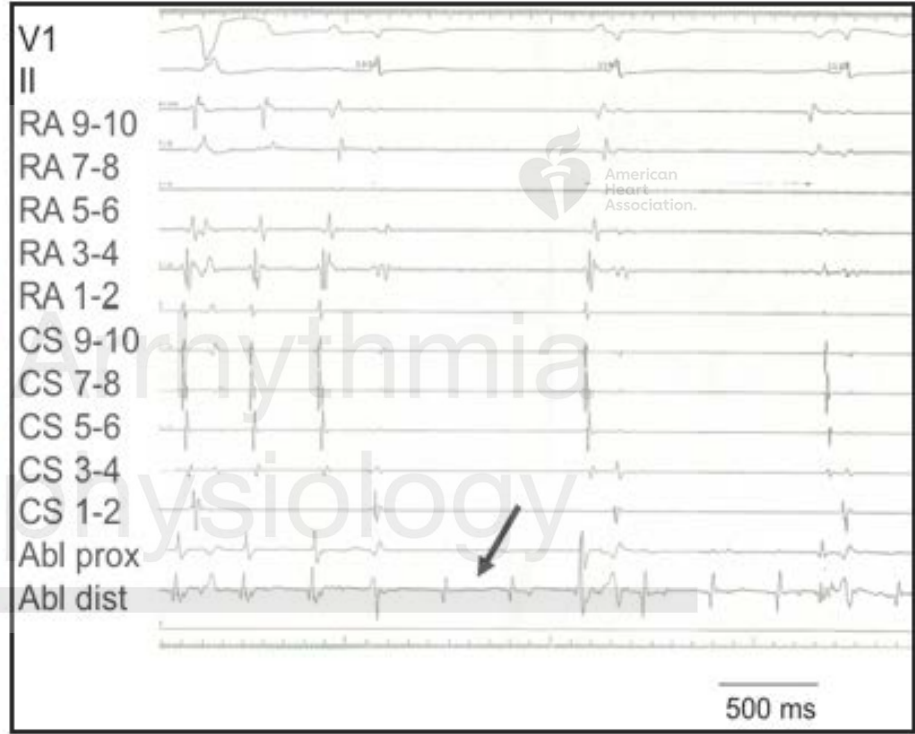
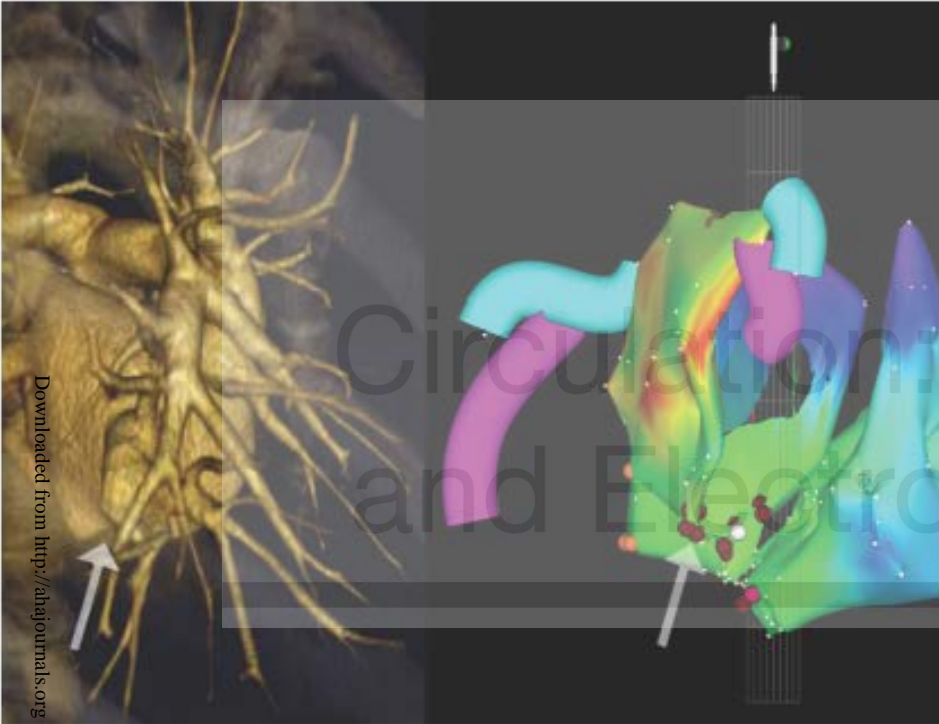


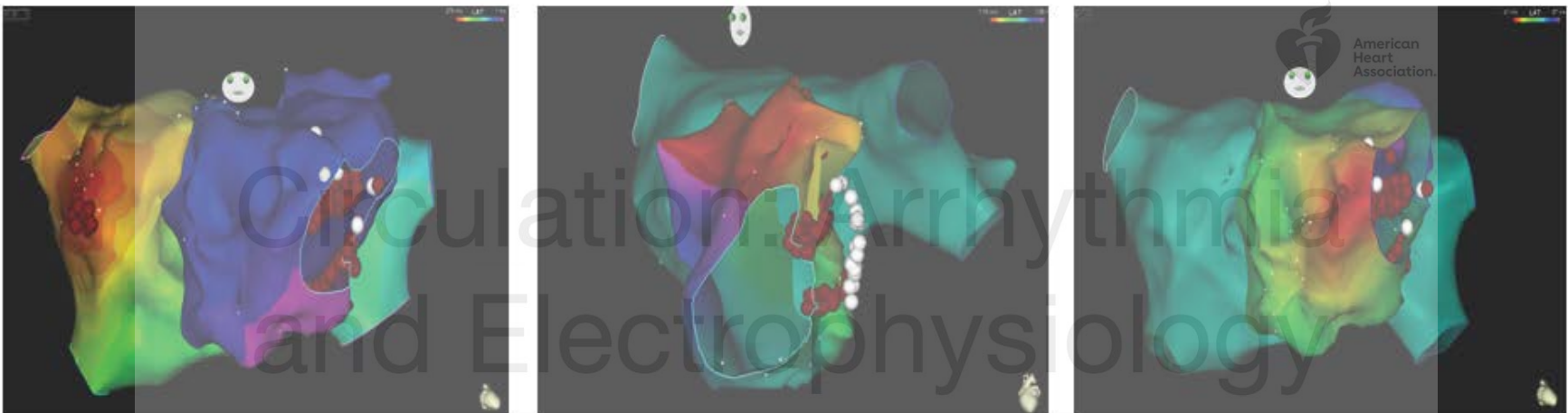
What the Study Adds?

- Our study confirmed functional recipient-to donor atrio-atrial connections in 21% of orthotopic heart transplant recipients presenting with atrial tachyarrhythmias. Immune privilege, characterized by the absence of donor specific antibodies, may facilitate development of these atrio-atrial connections.
- Computational modeling showed propagation across an atrio-atrial connection requires an isthmus width of ≥ 2 mm and conduction is cycle length and location dependent.
- Heart transplant patients with atrio-atrial connections tend to present with recipient focal atrial tachycardias or atrial fibrillation, propagating to the donor atria via the atrio-atrial connection, while patients without connections present with donor atrial arrhythmias, most commonly cavo-tricuspid isthmus dependent atrial flutter.

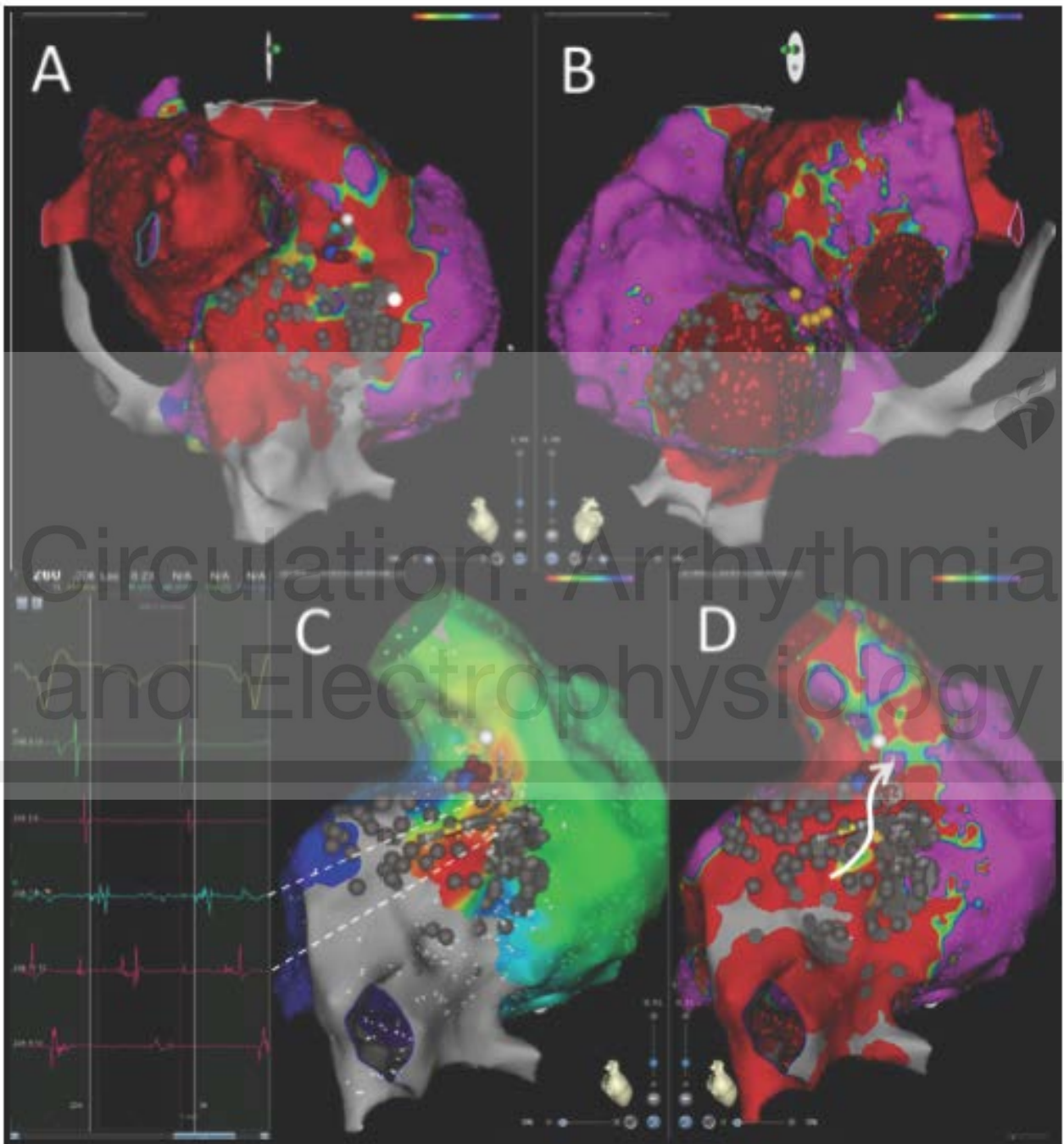






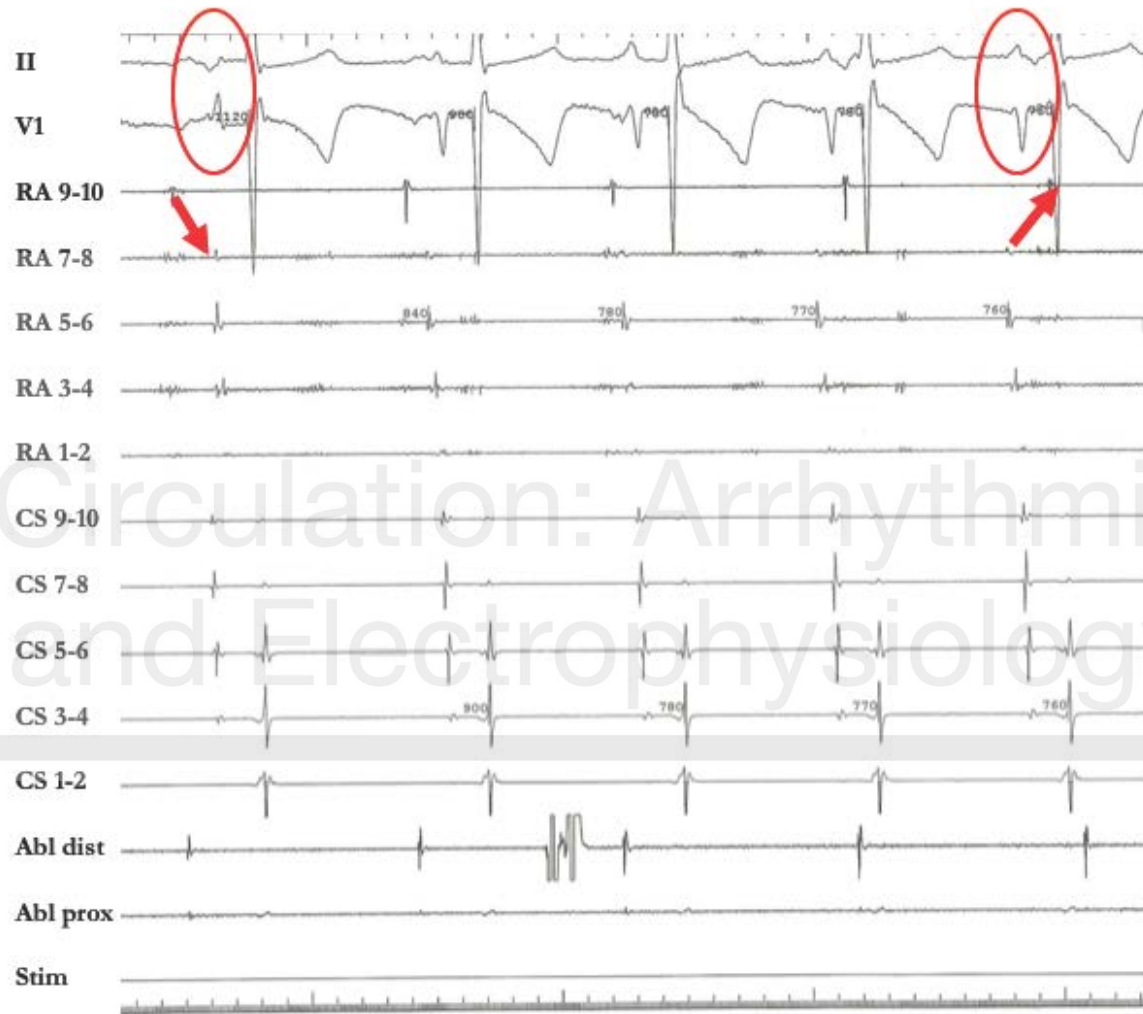


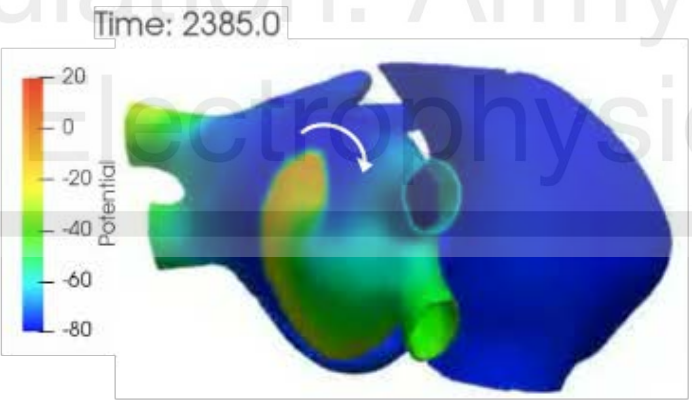
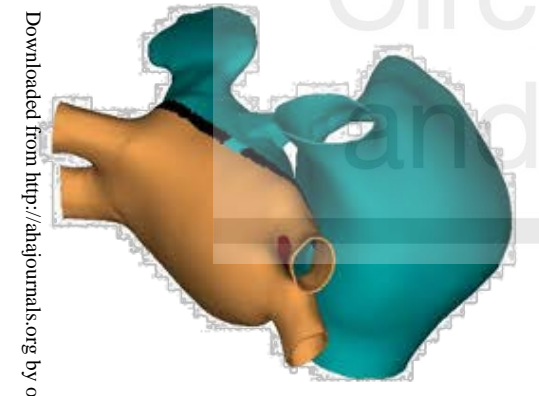
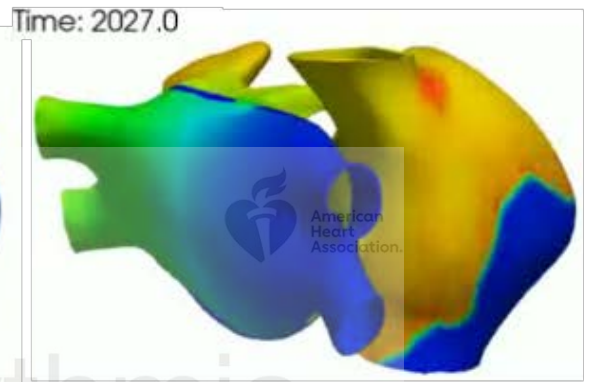
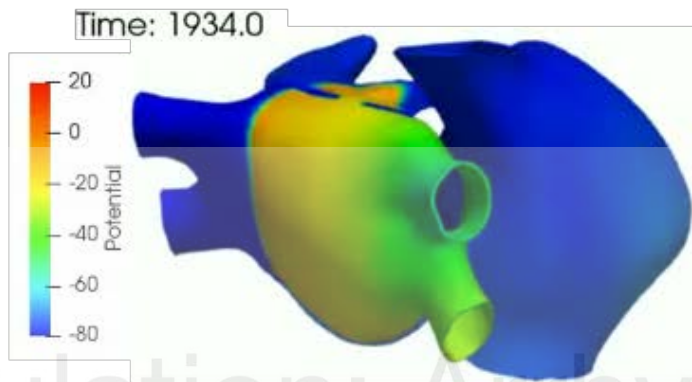
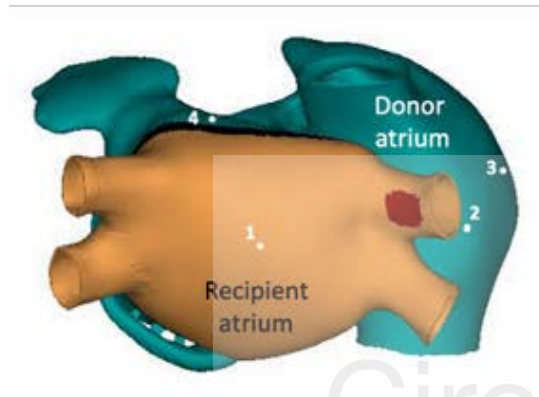
Circulation: Arrhythmia
and Electrophysiology



American Heart Association.

Circulation: Arrhythmia and Electrophysiology





Circulation: Arrhythmia and Electrophysiology